Skeletal Muscle

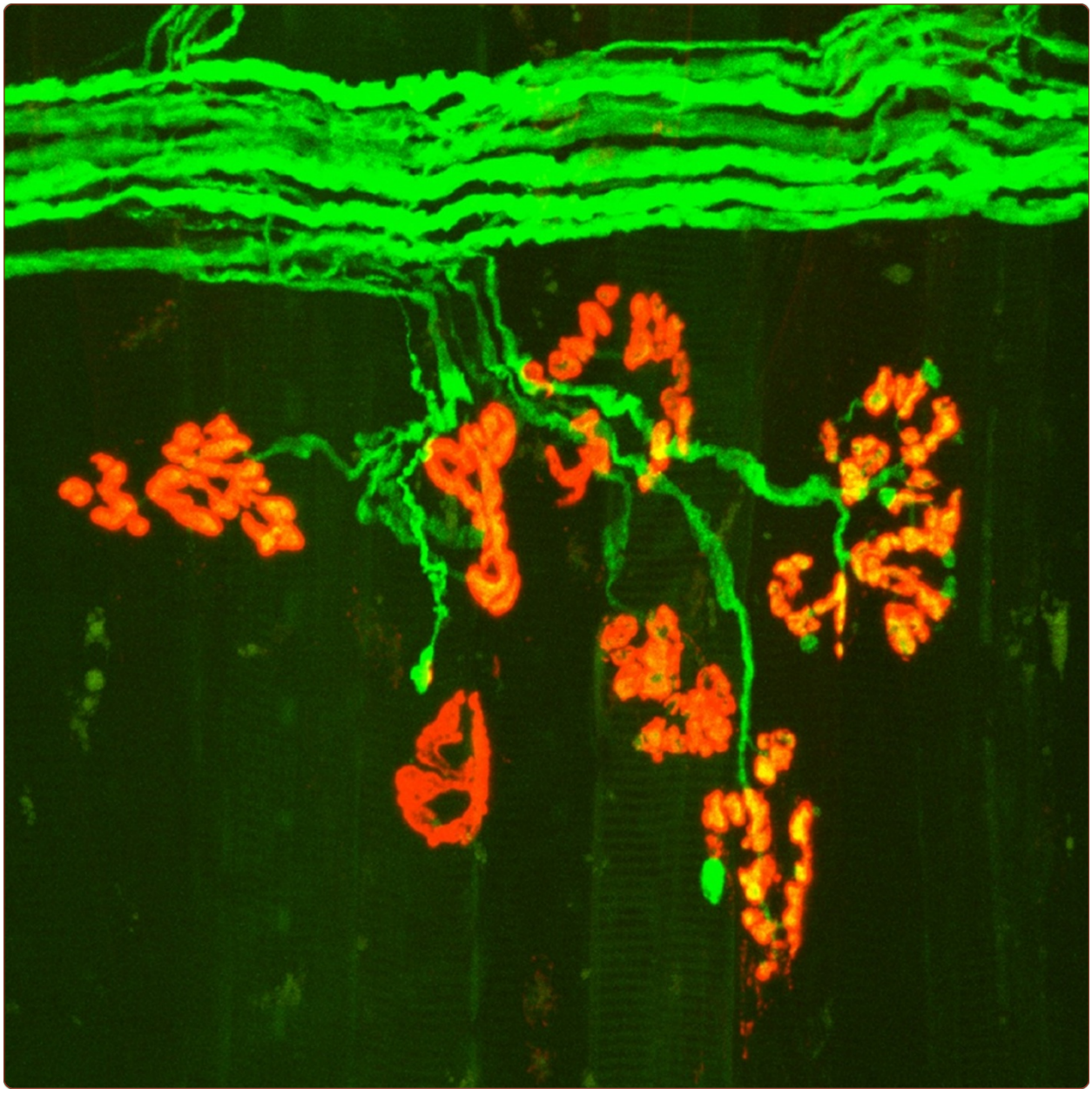

Myofiber branching rather than myofiber hyperplasia contributes to muscle hypertrophy in *mdx* mice

Faber *et al.*

BioMed Central

Faber *et al. Skeletal Muscle* 2014, **4**:10
http://www.skeletalmusclejournal.com/content/4/1/10

Faber et al. Skeletal Muscle 2014, 4:10
http://www.skeletalmusclejournal.com/content/4/1/10

Skeletal Muscle

RESEARCH Open Access

Myofiber branching rather than myofiber hyperplasia contributes to muscle hypertrophy in *mdx* mice

Rachel M Faber[1], John K Hall[1], Jeffrey S Chamberlain[1,2,3] and Glen B Banks[1*]

Abstract

Background: Muscle hypertrophy in the *mdx* mouse model of Duchenne muscular dystrophy (DMD) can partially compensate for the loss of dystrophin by maintaining peak force production. Histopathology examination of the hypertrophic muscles suggests the hypertrophy primarily results from the addition of myofibers, and is accompanied by motor axon branching. However, it is unclear whether an increased number of innervated myofibers (myofiber hyperplasia) contribute to muscle hypertrophy in the *mdx* mice.

Methods: To better understand the cellular mechanisms of muscle hypertrophy in *mdx* mice, we directly compared the temporal progression of the dystrophic pathology in the extensor digitorum longus (EDL) muscle to myofiber number, myofiber branching, and innervation, from 3 to 20 weeks of age.

Results: We found that a 28% increase in the number of fibers in transverse sections of muscle correlated with a 31% increase in myofiber branching. Notably, the largest increases in myofiber number and myofiber branching occurred after 12 weeks of age when the proportion of myofibers with central nuclei had stabilized and the *mdx* mouse had reached maturity. The dystrophic pathology coincided with profound changes to innervation of the muscles that included temporary denervation of necrotic fibers, fragmentation of synapses, and ultra-terminal axon sprouting. However, there was little evidence of synapse formation in the *mdx* mice from 3 to 20 weeks of age. Only 4.4% of neuromuscular junctions extended ultra-terminal synapses, which failed to mature, and the total number of neuromuscular junctions remained constant.

Conclusions: Muscle hypertrophy in *mdx* mice results from myofiber branching rather than myofiber hyperplasia.

Keywords: Duchenne muscular dystrophy, Skeletal muscle, Hypertrophy, Fiber branching, Innervation, Neuromuscular synapse, Inflammation

Background

Duchenne muscular dystrophy (DMD) is the most common dystrophy affecting approximately 1:4,000 boys, and is caused by mutations in the dystrophin gene [1,2]. A characteristic feature of DMD patients is the transitory hypertrophy of certain muscle groups, such as the gastrocnemius muscle. Direct correlations between computer tomography and histology of muscle biopsies demonstrate that an increase in myofiber number contributes to a transitory period of true hypertrophy in some DMD patients [3-5]. Ultimately, the failure of the muscle stem cells to continually regenerate the necrotic fibers leads, in part, to the replacement of muscle with adipose and connective tissue [6-9]. Muscle hypertrophy is found in most muscles in the *mdx* mouse model of DMD between 10 and 40 weeks of age and functionally compensates, in part, for the lack of dystrophin [5,10-13]. While the area of individual myofibers in *mdx* mice is highly variable, the average area is unchanged when compared to wild-type myofibers [14]. Similar to the DMD patients, estimations of myofiber number in transverse sections of *mdx* muscles are increased when compared to wild-type myofibers [12]. The endogenous mechanisms for increasing the number of myofibers is of considerable interest for muscle replacement strategies

* Correspondence: banksg@uw.edu
[1]Department of Neurology, University of Washington, Seattle, WA 98195-7720, USA
Full list of author information is available at the end of the article

BioMed Central

© 2014 Faber et al.; licensee BioMed Central Ltd. This is an Open Access article distributed under the terms of the Creative Commons Attribution License (http://creativecommons.org/licenses/by/4.0), which permits unrestricted use, distribution, and reproduction in any medium, provided the original work is properly credited. The Creative Commons Public Domain Dedication waiver (http://creativecommons.org/publicdomain/zero/1.0/) applies to the data made available in this article, unless otherwise stated.

to treat muscular dystrophy and sarcopenia. However, it is unclear whether the additional muscle results from myofiber branching and/or from the formation of new, innervated myofibers (myofiber hyperplasia).

Several considerations suggest that the increase in myofiber number in *mdx* mice could result from myofiber hyperplasia. Satellite cells associated with myofibers can begin proliferating and differentiate into new myotubes in culture [15]. Furthermore, proliferative expansion of an activated satellite cell *in vivo* can contribute to the regeneration of clusters of adjacent fibers [16-18]. Muscle necrosis in *mdx* mice can initiate the expression of growth-associated protein 43 (GAP43), a marker of axonal branching, in motor neurons [19]. While satellite cells are evenly distributed along a myofiber, a satellite cell resides in close proximity to the neuromuscular junction [20]. Innervation of regenerating fibers may be beneficial as direct stimulation of muscle can improve the engraftment of satellite cells [21]. Finally, myofibers can generate force through myomuscular junctions without having to extend from tendon to tendon [22]. Here, we directly compared the temporal progression of dystrophic pathology in mdx^{4cv} mice to innervation, myofiber number, and myofiber branching. Our results demonstrate that the increase in myofiber number in transverse sections of *mdx* EDL muscles results from myofiber branching rather than myofiber hyperplasia.

Methods

Mice

We generated the mdx^{4cv}: Thy1-CFP mice by breeding mdx^{4cv} C57Bl/6 females with C57Bl/6 mice homozygous for the Thy1-CFP transgene [23]. We utilized the male offspring, which were all mdx^{4cv} and expressed the CFP transgene under the control of the Thy1 promoter. For myofiber branching experiments we utilized mdx^{4cv} mice expressing the DsRed transgene in every cell. Mice were genotyped as previously described [24]. All experiments were performed in accordance with the guidelines approved by the Institutional Animal Care and Use Committee of the University of Washington.

Wholemount immunostaining

Wholemount immunostaining was performed as previously described [25]. Briefly, the mdx^{4cv}: Thy1-CFP mice were examined at 3 weeks (n = 4), 4 weeks (n = 4), 12 weeks (n = 6), and 20 weeks of age (n = 4). The mice were anesthetized with 2,2,2-tribromoethanol and perfused with 2% paraformaldehyde (PFA) in 1× phosphate buffered saline (PBS) by cardiac infusion. Cervical dislocation of the mouse was immediately followed by dissection of the lower limb such that the extensor digitorum longus (EDL) was the only muscle still attached to the bone and was incubated for 2 hours in 2% PFA at 4°C. The EDL muscles were excised from the bone and the distal tendons were isolated. The fascicular outlines of four muscle groups can be followed from tendon to tendon [26]. We stripped each of the four muscle groups that comprise the EDL using the distal tendons and retained the third group that normally inserts on the distal phalanx of the third digit of the foot. The third compartment of the EDL was incubated in 0.1 M glycine (in 1× PBS) for 1 hour and in blocking solution (1% BSA, 0.05% triton X-100, 1× PBS) overnight at 4°C. The muscles were then incubated in α-bungaratoxin conjugated to tetramethylrhodamine (TRITC; 1:800; Life Technologies) and GAP43 conjugated to DyLight 650 (1:800; Novus Biologicals) at room temperature on a rotating platform for 1 hour. For analyses of immune cells the muscles were incubated in Alexa-647 conjugated CD4, FITC-conjugated interferon-γ, Alexa488-conjugated CD8a, or FITC conjugated Mac-1 (1:50; BD Pharmingen). The muscles were then washed 3 × 10 min in 1× PBS and loaded onto superfrost^{+} slides with ProLong Gold antifade mounting medium containing 4′,6-diamidino-2-phenylindole (DAPI; Life Technologies). A composite image of the entire third muscle compartment was visualized and imaged using a Leica SP5 confocal microscope.

Quantitation of synapses

We quantitated the total number of synapses in the wholemount images using the count tool in Adobe Photoshop. Ultra-terminal branches were defined as motor axons that extended from the synapse. Those that terminated on an AChR cluster were labeled synaptic and those that did not terminate on an AChR cluster were labeled non-synaptic. The proportion of ultra-terminal synapses was calculated by dividing the total number of ultra-terminal synapses by the total number of neuromuscular junctions.

Quantitation of myofibers

Once the innervation of the third compartment of the EDL had been imaged the slide was incubated overnight in 2% paraformaldehyde in 1× PBS on a rotating table at room temperature to allow the coverslip to release from the slide without affecting the integrity of the muscle. The muscle was then placed in 20% sucrose for 2 hours at 4°C and frozen in OCT in 2-methylbutane in liquid N_2. Adjacent 10 μm sections were stained with hematoxilyn and eosin or wheat germ agglutinin (WGA) conjugated to fluorescein isothyocyanate (FITC; 1:100; Vector Laboratories). The sections stained with WGA were washed 3× 10 minutes in 1× PBS, mounted with ProLong Gold antifade mounting medium (Life Technologies). The sections were imaged using a Nikon Eclipse E1000 fluorescent microscope. The total number of myofibers in the third compartment of the EDL was quantitated using the slides stained with WGA using the count tool in Adobe photoshop. The myofiber areas were measured using the FIJI

computer software (NIH). We measured the areas of 167 myofibers from n = 4 wild-type mice and 265 myofibers from n = 4 *mdx* mice.

Analyses of branched fibers

The entire EDL muscles from *mdx*^{4cv}: DsRed mice aged 3 weeks, 4 weeks, 12 weeks, and 20 weeks were immediately digested in 6,000 Units of collagenase II (Worthington; NJ) for 60 minutes at 37°C with gentle agitation every 15 minutes. The collagenase II solution was exchanged with 1× PBS containing Alexa488-conjugated αBTX (1:800; Life Technologies) and incubated on a rotating table for 1 hour at room temperature. The muscles were washed three times in 1× PBS. The DsRed was expressed in every fiber, but quickly disappeared upon necrosis. The healthy DsRed fluorescing fibers were then carefully teased on a superfrost^{+} slide in ProLong Gold mounting medium containing DAPI. The fibers were quantitated and imaged using a Leica SP5 confocal microscope to gain sufficient resolution in the Z-direction as well as the X/Y planes. We quantitated 289 fibers at 3 weeks of age (n = 5), 256 fibers at 4 weeks (n = 3), 365 fibers at 12 weeks (n = 6), and 327 fibers at 20 weeks (n = 4). A myofiber with multiple branches was quantitated as a single branched myofiber. We also compared the myofiber diameters of unbranched (61 myofibers) and the combined diameters of branched myofibers (42 myofibers) in teased muscle preparations from n = 4, 5-month-old *mdx*^{4cv}: DsRed EDL using FIJI.

Statistics

Comparisons of muscle mass and myofiber areas were compared using a Students *t*-test. Myofiber number, ultra-terminal axon branches, and myofiber branching were analyzed using a one-way ANOVA with a Tukey post-test. Direct comparisons of synapse number with myofiber number were made using a two-way ANOVA with a Tukey post-test. All data analyses were performed using the PRISM software.

Results

Temporal progression of dystrophic pathology

To better understand the cellular mechanisms of muscle hypertrophy in *mdx* mice we directly compared the number of myofibers to the number of neuromuscular junctions. To visualize innervation of skeletal muscles we generated *mdx*^{4cv}: Thy1-CFP mice that express CFP in the motoneurons. We chose to examine the extensor digitorum longus (EDL) muscle as the anatomy of the EDL is well described [26]. The EDL has a single proximal tendon that attaches the lateral epicondyle of the distal femur to the distal phalanx of the foot through four distal tendons. The four muscle fascicles extend from tendon to tendon and can be easily and consistently separated. We chose the third muscle group because it is flat, small, and amenable to future muscle stem cell treatments.

Transverse sections of the third compartment of the wild-type: Thy1-CFP EDL revealed that less than 1% of the myofibers had centrally located nuclei, a marker of skeletal muscle regeneration (Figure 1A). Centrally located nuclei in the *mdx*^{4cv}: Thy1-CFP EDL were evident by 4 weeks of age (6% of muscles), while their numbers had peaked by 12 weeks (68%; P <0.001), and had stabilized until at least 20 weeks of age (68%; Figure 1). Thus, we chose 3 weeks (onset of necrosis), 4 weeks (evidence of regeneration), 12 weeks (peak of central nucleation), and 20 weeks (stabilization of dystrophic pathology) for the time points for this study. The third compartment of the EDL mass was increased by 82% in *mdx* compared to wild-type at 20 weeks of age (Figure 1C). While the myofiber areas were highly variable in the *mdx* mice at 20 weeks of age, the average areas remained unchanged (P = 0.71). Thus, the dystrophic pathology in the third compartment of the EDL led to significant hypertrophy in *mdx* mice, which did not result from changes in the average myofiber area.

Synaptic remodeling in mdx^{4cv}: Thy1-CFP mice

High-resolution confocal images of wholemount preparations of the third compartment of the EDL revealed that the motor nerve trunk traverses the skeletal myofibers to innervate the postsynaptic acetylcholine receptor (AChR) clusters (Figure 2A). The transgenic expression of CFP does not influence the innervation patterns in mice [23]. The innervation patterns were qualitatively normal when comparing wild-type and *mdx*^{4cv}: Thy1-CFP muscles at 4 weeks of age (Figure 2A). At 3 to 4 weeks of age we noticed a large number of small extrasynaptic AChR clusters within the *mdx*^{4cv}: Thy1-CFP muscles (Figure 2A). Detailed analyses of the wholemount preparations revealed that mononuclear inflammatory cells including activated CD4 positive T-helper cells expressing interferon-γ (Additional file 1: Figure S1A), CD8 positive cytotoxic T-lymphocytes (Additional file 1: Figure S1B), or macrophages (Additional file 1: Figure S1C) could express AChR, as previously described [27]. We found no direct association between the immune cells and the neuromuscular junctions.

The generation of new, innervated fibers requires synapse formation in the postnatal mice. Therefore, we performed a detailed examination of the wholemount preparations for evidence of synapse formation in *mdx*^{4cv}: Thy1-CFP EDL muscles. Neuromuscular junctions form as a plaque, and mature into a donut shape, and ultimately to a pretzel-like profile [28]. The presynaptic motor nerve terminal directly apposed the postsynaptic AChRs in wild-type muscles (Figure 2A) [29]. While the formation and maturation of the primary postsynaptic apparatus of the neuromuscular junction was normal in *mdx* mice (Figure 2A) [30], we

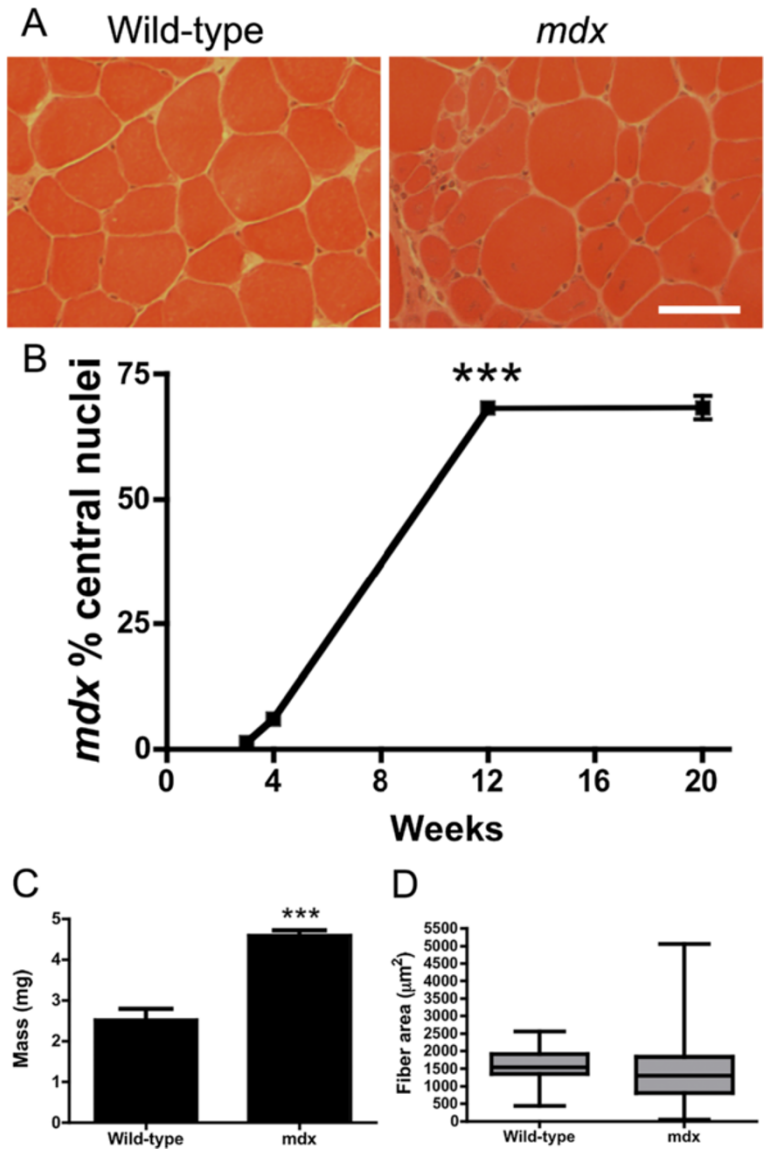

Figure 1 Progression of dystrophic histopathology in the third compartment of the extensor digitorum longus (EDL) muscle. (A) Hematoxylin and eosin stained frozen sections from 3-month-old wild-type and *mdx*^{4cv} muscle. Note the central nuclei in the *mdx*^{4cv} myofibers. Scale bar = 50 μm. **(B)** Proportion of central nuclei (+/- S.D.) in the third EDL compartment from 3 weeks to 20 weeks of age (n = 4-6). Note the apparent stabilization of dystrophic histopathology from 12 to 20 weeks of age. ***P <0.001 at 12 weeks compared to 4 weeks of age. At some time points, the standard deviation is too small to see. **(C)** The mass of the third compartment of the EDL at 20 weeks of age. P <0.001 compared to wild-type. **(D)** Box-whiskers plot of median +/- 75% of myofiber areas in wild-type and *mdx* mice at 20 weeks of age.

found that motor axons could extend beyond the synapse (ultra-terminal axon sprouting) (Figure 2B-E). On average, only 4.4% of the ultra-terminal axon sprouts innervated immature secondary synaptic plaques (Figure 2B). The number of ultra-terminal synapses reduced from approximately 16 per muscle (5.1%) at 3 weeks of age to approximately 12 per muscle (3.9%) at 20 weeks of age in *mdx* mice ($P = 0.056$; one-way ANOVA; Figure 2C). Furthermore, we found no evidence for the maturation of the ultra-terminal synaptic plaques to a donut or pretzel profile in any of the muscles examined. Most ultra-terminal axon sprouts in *mdx*^{4cv}: Thy1-CFP muscles did not terminate on to AChR clusters (Figure 2D, E). Non-synaptic ultra-terminal axon sprouts significantly increased with age, with approximately one per muscle at 3 weeks of age up to approximately 47 per muscle at 20 weeks of age (Figure 2D, E; P <0.01; one-way ANOVA). Thus, ultra-terminal synapse formation was evident in the *mdx* EDL muscles, but they were few in number, decreased with age, and failed to mature.

GAP43 is expressed in newly growing motor axons, terminal Schwann cells, immune cells, and parasympathetic

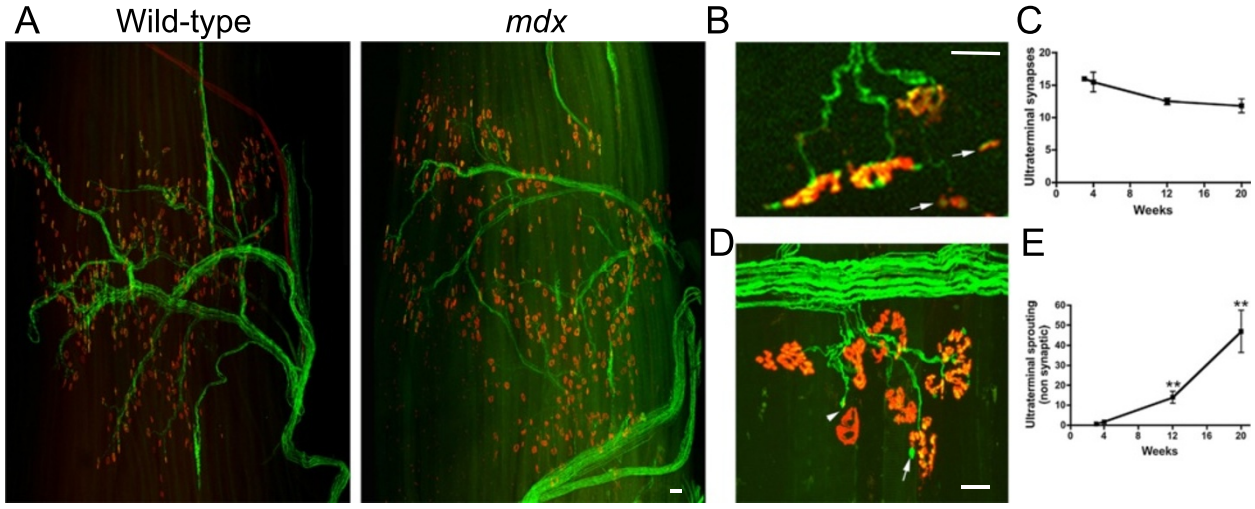

Figure 2 Innervation in the third EDL compartment. (A) The transgenic cyan fluorescence protein expression in neurons is pseudo-colored in green to demonstrate the innervation patterns in wild-type and mdx^{4cv} muscles at 4 weeks of age. Note the profound infiltration of small acetylcholine receptor (AChR) patches in synaptic and non-synaptic regions within the mdx^{4cv} muscles. Scale bar = 100 μm. **(B)** Shown are examples of ultra-terminal synapses (arrows) in 4-week-old muscle. Note that the ultra-terminal synapses are immature plaques. **(C)** Graph shows the mean +/- S.D. total number of ultra-terminal synapses demonstrating a modest reduction with age ($P = 0.056$; n = 4-6). **(D)** Shown is an example of denervation (arrow head) and non-synaptic ultra-terminal branching (arrow) in 20-week-old muscle. **(E)** The mean +/- S.D. total number of non-synaptic ultra-terminal branches increased with age (n = 4-6). $^{**}P < 0.01$ compared to 4 weeks of age. Scale bar for **B** and **D** = 30 μm.

nerves in blood vessels [19]. To determine if skeletal muscle necrosis in mdx^{4cv}: Thy1-CFP EDL muscles could initiate motor axon branching and synaptogenesis we examined the synapses at 3 and 4 weeks of age in whole-mount preparations. It is well established that synapses transition from the normal pretzel profile to the fragmented grape appearance upon muscle necrosis in *mdx* mice [30,31], but what happens in between to both the pre- and postsynaptic apparatus is unclear. Here, we found that the onset of skeletal muscle necrosis, as determined by Alexa488-IgG positive fibers, led normal pretzel profiled synapses (for example, Figure 3, synapse 1) to express GAP43 in the presynaptic nerve terminals (for example, Figure 3, synapse 2, 3, and 4). The early stage of necrosis, as determined by the localization of IgG on the surface of the muscle without overt cellular infiltrates, was accompanied by the retraction of the presynaptic nerve terminal from the postsynaptic apparatus (for example, Figure 3, synapse 3). The GAP43 in synapse 3 is expressed in the terminal Schwann cell, as previously described [19]. Infiltration of mononuclear cells into the necrotic myofibers led to the loss of the postsynaptic AChR clusters and the presynaptic nerve terminal (for example, Figure 3, synapse 4). Another example of the loss of innervation can be found in Figure 2D (arrow head). The regenerating fibers, as determined by the central nucleation without surface localized IgG, were reinnervated with a fragmented grape-profiled pre- and postsynaptic apparatus (for example, Figure 3, synapse 5). Thus, skeletal muscle necrosis in mdx^{4cv}: Thy1-CFP EDL muscles initiated a temporary

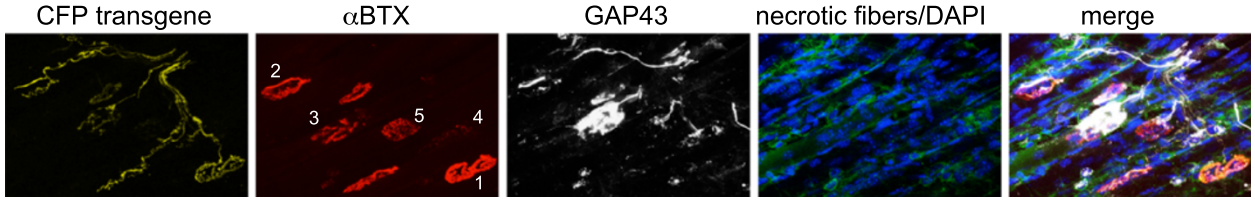

Figure 3 Skeletal muscle necrosis initiates temporary denervation. The CFP is pseudo-colored in yellow to allow the visualization of multiple fluorophores. Necrotic IgG positive fibers are shown in green. Note we numbered the synapses in the second panel. Synapse 1: Normal synapse in a non-necrotic fiber (no IgG). Synapse 2: Expression of GAP43 in a pre-necrotic fiber (IgG is next to the fiber). Synapse 3: Onset of necrosis (green fiber without overt cellular infiltrate) leads to the activation of the Schwann cell expressing GAP43 that retracts the presynaptic nerve terminal from the postsynaptic acetylcholine receptors. Synapse 4: Infiltration of cells into the necrotic fibers led to complete retraction of the nerve and loss of the AChR clusters. Synapse 5: Re-innervation of a fragmented postsynaptic synapse in a post-necrotic fiber (note the central nuclei and absence of IgG (green)). Scale bar = 30 μm.

denervation of the myofibers rather than directly evoking motor axon branching from the nerve terminals.

Direct comparison of myofiber number to innervation

The number of myofibers and the number of neuromuscular junctions in the wild-type EDL remains constant in maturing wild-type mice [32] (Additional file 2: Figure S2). Despite the profound changes in motor axon plasticity in the *mdx*^{4cv}: Thy1-CFP EDL muscles, we found no significant change in the total number of neuromuscular synapses from 3 weeks to 20 weeks of age (Figure 4; $P = 0.65$ one-way ANOVA). To directly compare the number of synapses to the number of myofibers we reprocessed the same EDL muscle compartment for histological sections and stained the sections with wheat germ agglutinin conjugated to fluorescein isothyocyanate (FITC). We examined sections through the mid-belly of the EDL to coincide with the placement of the synapses. Quantitation of the total number of *mdx*^{4cv}: Thy1-CFP myofibers revealed a 28% increase from 3 weeks to 20 weeks of age (Figure 4; $P < 0.001$; one-way ANOVA). Interestingly, the total number of fibers increased by 19% from 12 weeks to 20 weeks of age when the dystrophic histopathology had seemingly stabilized (Figure 1). Thus, an increase in myofiber number in hypertrophic *mdx* muscles was not accompanied by a change in the total number of neuromuscular junctions.

Increased myofiber numbers in *mdx*^{4cv}: Thy1-CFP mice result from myofiber branching

We next examined whether the increase in myofiber number in transverse sections of the third compartment of the *mdx*^{4cv}: Thy1-CFP EDL muscles correlated with an increase in myofiber branching. Here, we digested the entire *mdx*^{4cv}: Thy1-CFP EDL muscles with collagenase II and quantitated the proportion of branched fibers (Figure 5). To easily count the muscles we utilized the *mdx*^{4cv}: Thy1-CFP expressing DsRed. We found three types of myofiber branching including branching from the middle of the myofiber (53% of myofibers with branches; Figure 5A), branches that re-entered the original myofiber (13% of myofibers with branches; Figure 5B), and myofiber branching at the ends of the myofiber (13% of myofibers with branches; Figure 5C). Of the myofibers with branches, 21% had multiple branch points (Figure 5D), with various combinations of the above. We found that the proportion of branched red myofibers increased from 2% at 3 weeks of age to 33% at 20 weeks of age (31% increase; $P < 0.001$; one-way ANOVA), which was consistent with the 28% increase in the number of fibers in transverse sections. Interestingly, the proportion of branched fibers increased by 21% between 12 weeks and 20 weeks of age (Figure 5E), when the dystrophic histopathology had stabilized (Figure 1). The combined average diameter of a branched myofiber was increased by 76% when compared to the unbranched *mdx* myofibers at 5 months of age demonstrating that myofiber branching led to myofiber hypertrophy (Figure 5F; $P < 0.001$). While we found that 1.4% of the unbranched fibers had multiple synapses (Additional file 3: Figure S3), all of the branched fibers were singularly innervated at all ages examined (Figure 5), as previously described [33]. Thus, the temporal increase in myofiber number in transverse sections of *mdx*^{4cv}: Thy1-CFP muscles directly correlated with the increased number of branched myofibers.

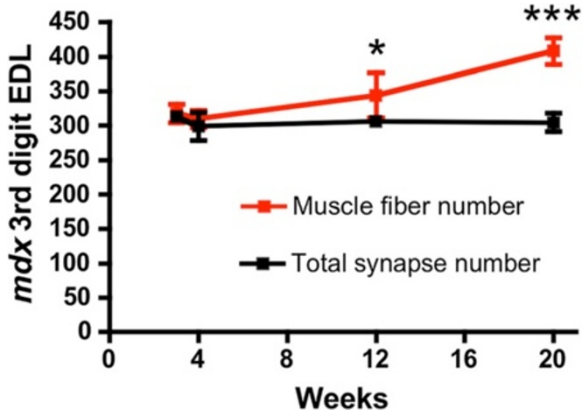

Figure 4 Direct comparison of myofiber number with synapse number in the third EDL compartment. Note that myofiber number in transverse sections increases with age while the synapse number remains unchanged (n = 4-6). *$P < 0.05$ and ***$P < 0.001$ fiber number compared to synapse number.

Discussion

The transitory muscle hypertrophy in *mdx* mice can lead to a partial functional compensation for the lack of dystrophin [5,10-13]. For example, larger muscles in *mdx* mice generate greater force than in wild-type mice, but they do not develop greater levels of specific force and they continue to display cycles of necrosis and regeneration [13]. Muscle necrosis leads to a potent regenerative response in *mdx* mice that leads to the functional hypertrophy [6-9]. To better understand the cellular mechanisms for muscle hypertrophy in *mdx* mice we directly compared the temporal progression of dystrophic pathology in the third compartment of the EDL in *mdx*^{4cv}: Thy1-CFP mice to myofiber number, innervation, and myofiber branching. Similar to previous studies we found an increase in the number of myofibers in transverse sections [12]. Despite profound changes to the innervation of *mdx* muscles, there was no change in the total number of neuromuscular junctions. Rather, the increase in myofiber number quantitated in transverse sections correlated with an increase in myofiber branching. Thus, our data suggest that myofiber branching rather than the formation of new,

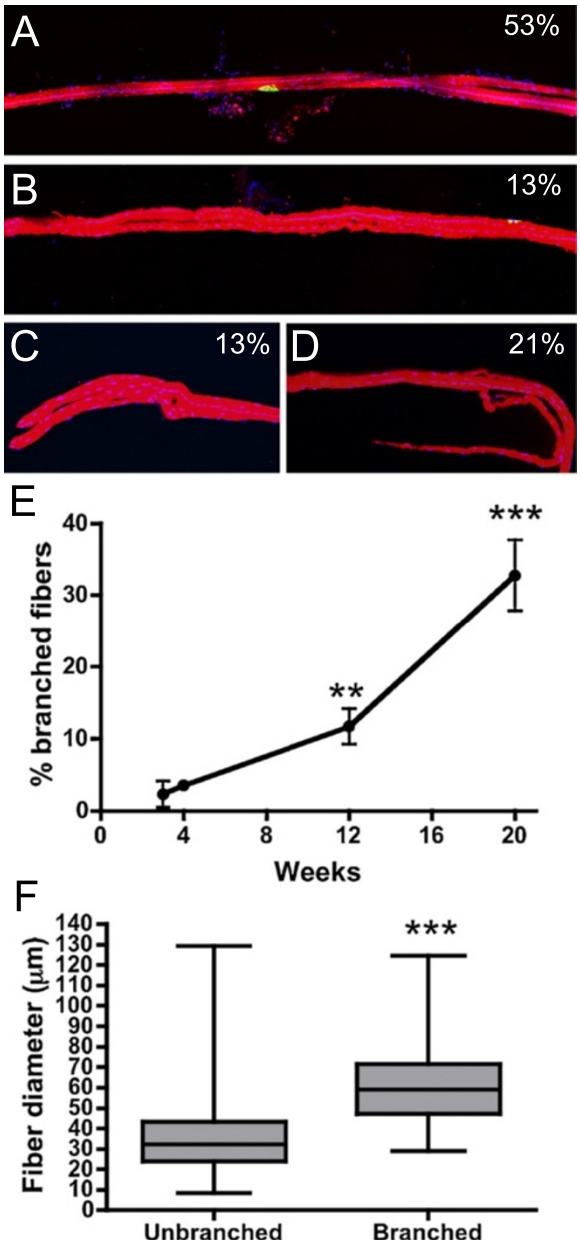

Figure 5 Myofiber branching in the EDL. (A) A singularly innervated branched myofiber expressing DsRed, DAPI in blue and AChR cluster in green. Scale bar = 50 μm. **(B)** Branches can also rejoin the initial fiber and/or **(C)** branch at the ends of myofibers. Percentages in the images in **A-C** show the proportion of myofibers with the respective branching phenotype. **(D)** Shown is an example of a myofiber with multiple branch points. Approximately 21% of myofibers with branches had multiple branch points. **(E)** Mean +/- S.D. of fiber branching increases with age. $^{**}P$ <0.01 compared to 4 weeks and $^{***}P$ <0.001 compared to 12 weeks (n = 4-6). **(F)** Median +/- 75% diameter of unbranched *mdx* EDL myofibers compared to the combined diameter of branched myofibers at 5 months of age. $^{***}P$ <0.001.

innervated myofibers (myofiber hyperplasia) contributes to the muscle hypertrophy in *mdx* mice.

Fiber branches can form through the generation of a new myofiber segment physically connected to a pre-existing myofiber or by splitting a fiber into two. Consistent with the former possibility, we found that all branched fibers in the *mdx* mice had central nuclei in at least one of the branches (Figure 5). Furthermore, fiber branches in *mdx* mice express developmental myosin [33]. Activated satellite cells could potentially generate the fiber branches by fusing into nascent or pre-existing myofibers in a non-linear pattern [34]. Satellite cells are also required for the increase in number of fibers that is associated with experimental induction of muscle hypertrophy by mechanical overload [35]. Our results confirm previous reports that the most severe dystrophic histopathology occurs during maturation of the mouse from 3 to 12 weeks of age [12,36-38]. Interestingly, the greatest changes in myofiber number and myofiber branching occurred between 12 and 20 weeks of age when cycles of necrosis and regeneration had reached a steady state level. The stabilization of dystrophic histopathology during this later period requires the activation of satellite cells to support myofiber regeneration [12]. Therefore, it is likely that the potent regenerative response in *mdx* muscles leads to hypertrophy through the generation of myofiber branches rather than forming entirely new innervated myofibers.

While skeletal muscle necrosis can lead to overt changes in GAP43 expression in *mdx* muscles [19], it was unclear whether this represented overt changes to innervation of the skeletal muscles because GAP43 can label multiple cell types. Our detailed examination of wholemount preparations demonstrated profound changes to the innervation of mdx^{4cv}: Thy1-CFP muscles. We found that GAP43 was expressed in the motor nerves and terminal Schwann cells during the temporary denervation of the necrotic fibers. The terminal Schwann cell normally envelops the motor nerve terminal when synapses are eliminated during early postnatal development [39]. A similar process in *mdx* mice could potentially function to protect the nerve terminal from the profound inflammatory response within the muscle [40]. Skeletal muscle necrosis did not directly elicit ultra-terminal axon sprouting, which was prevalent at all ages examined. Only a small portion of these axonal extensions formed ultra-terminal synaptic plaques, which never developed into the donut or pretzel profiles of maturing synapses. The non-synaptic ultra-terminal axon sprouting was most prevalent between 12 and 20 weeks of age similar to the time course of myofiber branching. The excitation-contraction coupling is disturbed in branched myofibers [33], and this could potentially impair synaptic transmission leading to the presynaptic axonal extensions. We found that branched myofibers

were singularly innervated, as previously described [33], demonstrating that multiple innervation did not influence the stability of the presynaptic terminals. We found no evidence of fiber branching between multiple fibers in the EDL like previously shown for the soleus muscle [41]. It would be interesting to examine whether a multi-syncytial reticulum could influence innervation of the *mdx* myofibers, as myofibers are normally singularly innervated. It is also unlikely that the ultra-terminal sprouting results from the absence of dystrophin within the central nervous system (CNS). Full-length dystrophin stabilizes GABAergic receptor clusters in the CNS [42]. However, impaired inhibitory innervation in adult mice would predictably increase motor nerve excitation and restriction of the motor axon branches [25]. Furthermore, the mdx^{4cv} mouse strain retains the truncated Dp116 dystrophin isoform in Schwann cells such that axon conductance is unlikely to be changed [43], and no myofiber abnormalities have been observed in transgenic *mdx* mice expressing full-length dystrophin only in striated muscle [44]. While the profound changes to innervation are an integral part of the dystrophic pathophysiology in *mdx* mice, we found no change in the total number of synapses that would be consistent with the formation of new, innervated myofibers.

Myofiber branching ensures that the developing myotubes are innervated irrespective of the site of injury. Considering the increased muscle in our study resulted almost entirely from myofiber branching, it is likely that myofiber branching helps to maintain the peak force capacity of *mdx* muscles [13]. While there are clear benefits of myofiber branching, the branch points in *mdx* mice are primary sites of calcium mishandling and contraction-induced injury [33,45-47]. Thus, it would be preferable to reverse muscle loss with the formation of entirely new, innervated myofibers. Multiple studies have suggested that prospective cellular therapies for DMD can form new fibers in *mdx* muscles. For instance, direct administration of fibroblasts genetically modified to form myofibers can form multiple dystrophin positive myotubes in mdx^{4cv} muscles, although it was not determined whether these were either innervated or attached to pre-existing myofibers [48]. Delivery of isolated satellite cells contributed to the regeneration of a myofiber that only expressed the donor GFP and not the recipient DsRed [49]. Transplantation of myogenic progenitors derived from induced pluripotent stem cells can also contribute to innervated fibers within the recipient [50]. We also found that myofiber transplantation increased the number of myofibers in transverse sections of aged (28-32 months) tibialis anterior muscles [51]. However, none of these studies demonstrated that the donor cells formed a whole innervated myofiber without the contribution from the endogenous host cells. Our current study demonstrates that the formation of new, innervated myofibers is not a natural process of muscle regeneration in the mdx^{4cv} mice. However, it remains important to examine whether various experimental manipulations utilizing diverse prospective cellular therapies and delivery techniques can form new, innervated muscle fibers, which could be important for reversing the loss of muscle mass in older DMD patients.

Conclusions

Muscle hypertrophy is a transitory feature of some muscles in DMD and is a prevalent phenotype of the *mdx* mouse model of DMD. Analysis of muscle histopathology suggests the formation of new myofibers contributes to the hypertrophy. New myofibers require innervation to survive. However, it is not clear whether the regenerative response to muscle necrosis in *mdx* mice leads to the formation of new, innervated myofibers. Here, we demonstrate that the new muscle receives innervation by branching from the existing myofibers, rather than directly from the motoneuron. Furthermore, the propensity of myofibers to branch increased once the *mdx* mouse had reached maturity. These results have important implications for muscle replacement strategies for muscular dystrophy and sarcopenia.

Additional files

Additional file 1: Figure S1. Detailed examination of the small AChR patches revealed them to be either **(A)** activated CD4 T-helper lymphocytes expressing interferon-γ, **(B)** CD8 cytotoxic T lymphocytes, or most prominently **(C)** macrophages. The CFP is pseudo-colored in yellow in **A-C** to allow the presentation of multiple fluorophores. We found no direct association between the immune cells and the synapse. Scale bars for **A-C** = 30 μm.

Additional file 2: Figure S2. Synapse numbers in the third compartment of the EDL in wild-type mice does not change between 4 weeks and 12 weeks of age (n = 4).

Additional file 3: Figure S3. Shown are **(A)** a singularly innervated myofiber and **(B)** an example of a rare myofiber with multiple synapses.

Abbreviations

CFP: Cyan fluorescence protein; DMD: Duchenne muscular dystrophy; EDL: Extensor digitorum longus; GAP 43: Growth associated protein 43; PBS: Phosphate buffered saline.

Competing interests

The authors declare they have no competing interests.

Authors' contributions

RMF contributed to experimental design, performed experiments, and helped draft the manuscript. JKH imaged the 5-month *mdx* innervation and edited the manuscript. JSC contributed resources and edited the manuscript. GBB conceived the project, contributed to all experimental designs, performed experiments, and helped draft and edit the manuscript. All authors read and approved the final manuscript.

Acknowledgements

This work was supported by grants from the MDA and AHA (to GBB) and NIH grant AR40864 (JSC).

Author details

[1]Department of Neurology, University of Washington, Seattle, WA 98195-7720, USA. [2]Department of Biochemistry, University of Washington,

Seattle, WA 98195-7720, USA. [3]Department of Medicine, University of Washington, Seattle, WA 98195-7720, USA.

Received: 30 March 2014 Accepted: 6 May 2014
Published: 23 May 2014

References

1. Hoffman EP, Brown RH Jr, Kunkel LM: **Dystrophin: the protein product of the Duchenne muscular dystrophy locus.** *Cell* 1987, **51:**919–928.
2. Koenig M, Hoffman EP, Bertelson CJ, Monaco AP, Feener C, Kunkel LM: **Complete cloning of the Duchenne muscular dystrophy (DMD) cDNA and preliminary genomic organization of the DMD gene in normal and affected individuals.** *Cell* 1987, **50:**509–517.
3. Jones DA, Round JM, Edwards RH, Grindwood SR, Tofts PS: **Size and composition of the calf and quadriceps muscles in Duchenne muscular dystrophy. A tomographic and histochemical study.** *J Neurol Sci* 1983, **60:**307–322.
4. Reimers CD, Schlotter B, Eicke BM, Witt TN: **Calf enlargement in neuromuscular diseases: a quantitative ultrasound study in 350 patients and review of the literature.** *J Neurol Sci* 1996, **143:**46–56.
5. Kornegay JN, Childers MK, Bogan DJ, Bogan JR, Nghiem P, Wang J, Fan Z, Howard JF Jr, Schatzberg SJ, Dow JL, Grange RW, Styner MA, Hoffman EP, Wagner KR: **The paradox of muscle hypertrophy in muscular dystrophy.** *Phys Med Rehabil Clin N Am* 2012, **23:**149–172. xii.
6. Blau HM, Webster C, Pavlath GK: **Defective myoblasts identified in Duchenne muscular dystrophy.** *Proc Natl Acad Sci U S A* 1983, **80:**4856–4860.
7. Webster C, Blau HM: **Accelerated age-related decline in replicative life-span of Duchenne muscular dystrophy myoblasts: implications for cell and gene therapy.** *Somat Cell Mol Genet* 1990, **16:**557–565.
8. Mouly V, Aamiri A, Bigot A, Cooper RN, Di Donna S, Furling D, Gidaro T, Jacquemin V, Mamchaoui K, Negroni E, Perie S, Renault V, Silva-Barbosa SD, Butler-Browne GS: **The mitotic clock in skeletal muscle regeneration, disease and cell mediated gene therapy.** *Acta Physiol Scand* 2005, **184:**3–15.
9. Sacco A, Mourkioti F, Tran R, Choi J, Llewellyn M, Kraft P, Shkreli M, Delp S, Pomerantz JH, Artandi SE, Blau HM: **Short telomeres and stem cell exhaustion model Duchenne muscular dystrophy in mdx/mTR mice.** *Cell* 2010, **143:**1059–1071.
10. Coulton GR, Curtin NA, Morgan JE, Partridge TA: **The mdx mouse skeletal muscle myopathy: II, Contractile properties.** *Neuropathol Appl Neurobiol* 1988, **14:**299–314.
11. Coulton GR, Morgan JE, Partridge TA, Sloper JC: **The mdx mouse skeletal muscle myopathy: I. A histological, morphometric and biochemical investigation.** *Neuropathol Appl Neurobiol* 1988, **14:**53–70.
12. Pagel CN, Partridge TA: **Covert persistence of mdx mouse myopathy is revealed by acute and chronic effects of irradiation.** *J Neurol Sci* 1999, **164:**103–116.
13. Lynch GS, Hinkle RT, Chamberlain JS, Brooks SV, Faulkner JA: **Force and power output of fast and slow skeletal muscles from mdx mice 6–28 months old.** *J Physiol* 2001, **535:**591–600.
14. Banks GB, Judge LM, Allen JM, Chamberlain JS: **The polyproline site in hinge 2 influences the functional capacity of truncated dystrophins.** *PLoS Genet* 2010, **6:**e1000958.
15. Bockhold KJ, Rosenblatt JD, Partridge TA: **Aging normal and dystrophic mouse muscle: analysis of myogenicity in cultures of living single fibers.** *Muscle Nerve* 1998, **21:**173–183.
16. Crawford GE, Lu QL, Partridge TA, Chamberlain JS: **Suppression of revertant fibers in mdx mice by expression of a functional dystrophin.** *Hum Mol Genet* 2001, **10:**2745–2750.
17. Yokota T, Lu QL, Morgan JE, Davies KE, Fisher R, Takeda S, Partridge TA: **Expansion of revertant fibers in dystrophic mdx muscles reflects activity of muscle precursor cells and serves as an index of muscle regeneration.** *J Cell Sci* 2006, **119:**2679–2687.
18. Sacco A, Doyonnas R, Kraft P, Vitorovic S, Blau HM: **Self-renewal and expansion of single transplanted muscle stem cells.** *Nature* 2008, **456:**502–506.
19. Verze L, Buffo A, Rossi F, Oestreicher AB, Gispen WH, Strata P: **Increase of B-50/GAP-43 immunoreactivity in uninjured muscle nerves of MDX mice.** *Neuroscience* 1996, **70:**807–815.
20. Snow MH: **Satellite cell distribution within the soleus muscle of the adult mouse.** *Anat Rec* 1981, **201:**463–469.
21. Distefano G, Ferrari RJ, Weiss C, Deasy BM, Boninger ML, Fitzgerald GK, Huard J, Ambrosio F: **Neuromuscular electrical stimulation as a method to maximize the beneficial effects of muscle stem cells transplanted into dystrophic skeletal muscle.** *PLoS One* 2013, **8:**e54922.
22. Hijikata T, Ishikawa H: **Functional morphology of serially linked skeletal muscle fibers.** *Acta Anat (Basel)* 1997, **159:**99–107.
23. Feng G, Mellor RH, Bernstein M, Keller-Peck C, Nguyen QT, Wallace M, Nerbonne JM, Lichtman JW, Sanes JR: **Imaging neuronal subsets in transgenic mice expressing multiple spectral variants of GFP.** *Neuron* 2000, **28:**41–51.
24. Banks GB, Combs AC, Chamberlain JS: **Sequencing protocols to genotype mdx, mdx(4cv), and mdx(5cv) mice.** *Muscle Nerve* 2010, **42:**268–270.
25. Banks GB, Kanjhan R, Wiese S, Kneussel M, Wong LM, O'Sullivan G, Sendtner M, Bellingham MC, Betz H, Noakes PG: **Glycinergic and GABAergic synaptic activity differentially regulate motoneuron survival and skeletal muscle innervation.** *J Neurosci* 2005, **25:**1249–1259.
26. Balice-Gordon RJ, Thompson WJ: **The organization and development of compartmentalized innervation in rat extensor digitorum longus muscle.** *J Physiol* 1988, **398:**211–231.
27. Leite PE, Lagrota-Candido J, Moraes L, D'Elia L, Pinheiro DF, da Silva RF, Yamasaki EN, Quirico-Santos T: **Nicotinic acetylcholine receptor activation reduces skeletal muscle inflammation of mdx mice.** *J Neuroimmunol* 2010, **227:**44–51.
28. Marques MJ, Conchello JA, Lichtman JW: **From plaque to pretzel: fold formation and acetylcholine receptor loss at the developing neuromuscular junction.** *J Neurosci* 2000, **20:**3663–3675.
29. Deschenes MR, Hurst TE, Ramser AE, Sherman EG: **Presynaptic to postsynaptic relationships of the neuromuscular junction are held constant across age and muscle fiber type.** *Dev Neurobiol* 2013, **73:**744–753.
30. Lyons PR, Slater CR: **Structure and function of the neuromuscular junction in young adult mdx mice.** *J Neurocytol* 1991, **20:**969–981.
31. Banks GB, Chamberlain JS, Froehner SC: **Truncated dystrophins can influence neuromuscular synapse structure.** *Mol Cell Neurosci* 2009, **40:**433–441.
32. White RB, Bierinx AS, Gnocchi VF, Zammit PS: **Dynamics of muscle fibre growth during postnatal mouse development.** *BMC Dev Biol* 2010, **10:**21.
33. Lovering RM, Michaelson L, Ward CW: **Malformed mdx myofibers have normal cytoskeletal architecture yet altered EC coupling and stress-induced Ca2+ signaling.** *Am J Physiol Cell Physiol* 2009, **297:**C571–C580.
34. Anderson JE: **A role for nitric oxide in muscle repair: nitric oxide-mediated activation of muscle satellite cells.** *Mol Biol Cell* 2000, **11:**1859–1874.
35. McCarthy JJ, Mula J, Miyazaki M, Erfani R, Garrison K, Farooqui AB, Srikuea R, Lawson BA, Grimes B, Keller C, Van Zant G, Campbell KS, Esser KA, Dupont-Versteedgen EE, Peterson CA: **Effective fiber hypertrophy in satellite cell-depleted skeletal muscle.** *Development* 2011, **138:**3657–3666.
36. Pastoret C, Sebille A: **Age-related differences in regeneration of dystrophic (mdx) and normal muscle in the mouse.** *Muscle Nerve* 1995, **18:**1147–1154.
37. Pastoret C, Sebille A: **mdx mice show progressive weakness and muscle deterioration with age.** *J Neurol Sci* 1995, **129:**97–105.
38. Partridge TA: **The mdx mouse model as a surrogate for Duchenne muscular dystrophy.** *FEBS J* 2013, **280:**4177–4186.
39. Bishop DL, Misgeld T, Walsh MK, Gan WB, Lichtman JW: **Axon branch removal at developing synapses by axosome shedding.** *Neuron* 2004, **44:**651–661.
40. Vetrone SA, Montecino-Rodriguez E, Kudryashova E, Kramerova I, Hoffman EP, Liu SD, Miceli MC, Spencer MJ: **Osteopontin promotes fibrosis in dystrophic mouse muscle by modulating immune cell subsets and intramuscular TGF-beta.** *J Clin Invest* 2009, **119:**1583–1594.
41. Tamaki T, Sekine T, Akatsuka A, Uchiyama S, Nakano S: **Three-dimensional cytoarchitecture of complex branched fibers in soleus muscle from mdx mutant mice.** *Anat Rec* 1993, **237:**338–344.
42. Knuesel I, Mastrocola M, Zuellig RA, Bornhauser B, Schaub MC, Fritschy JM: **Short communication: altered synaptic clustering of GABAA receptors in mice lacking dystrophin (mdx mice).** *Eur J Neurosci* 1999, **11:**4457–4462.
43. Banks GB, Chamberlain JS: **The value of mammalian models for duchenne muscular dystrophy in developing therapeutic strategies.** *Curr Top Dev Biol* 2008, **84:**431–453.
44. Cox GA, Cole NM, Matsumura K, Phelps SF, Hauschka SD, Campbell KP, Faulkner JA, Chamberlain JS: **Overexpression of dystrophin in transgenic mdx mice eliminates dystrophic symptoms without toxicity.** *Nature* 1993, **364:**725–729.

45. Chan S, Head SI, Morley JW: **Branched fibers in dystrophic mdx muscle are associated with a loss of force following lengthening contractions.** *Am J Physiol Cell Physiol* 2007, **293:**C985–C992.
46. Chan S, Head SI: **The role of branched fibres in the pathogenesis of Duchenne muscular dystrophy.** *Exp Physiol* 2011, **96:**564–571.
47. Head SI: **Branched fibres in old dystrophic mdx muscle are associated with mechanical weakening of the sarcolemma, abnormal Ca2+ transients and a breakdown of Ca2+ homeostasis during fatigue.** *Exp Physiol* 2010, **95:**641–656.
48. Kimura E, Han JJ, Li S, Fall B, Ra J, Haraguchi M, Tapscott SJ, Chamberlain JS: **Cell-lineage regulated myogenesis for dystrophin replacement: a novel therapeutic approach for treatment of muscular dystrophy.** *Hum Mol Genet* 2008, **17:**2507–2517.
49. Cerletti M, Jurga S, Witczak CA, Hirshman MF, Shadrach JL, Goodyear LJ, Wagers AJ: **Highly efficient, functional engraftment of skeletal muscle stem cells in dystrophic muscles.** *Cell* 2008, **134:**37–47.
50. Filareto A, Parker S, Darabi R, Borges L, Iacovino M, Schaaf T, Mayerhofer T, Chamberlain JS, Ervasti JM, McIvor RS, Kyba M, Perlingeiro RC: **An ex vivo gene therapy approach to treat muscular dystrophy using inducible pluripotent stem cells.** *Nat Commun* 2013, **4:**1549.
51. Hall JK, Banks GB, Chamberlain JS, Olwin BB: **Prevention of muscle aging by myofiber-associated satellite cell transplantation.** *Sci Transl Med* 2010, **2:**57ra–83ra.

doi:10.1186/2044-5040-4-10
Cite this article as: Faber *et al.*: Myofiber branching rather than myofiber hyperplasia contributes to muscle hypertrophy in *mdx* mice. *Skeletal Muscle* 2014 **4**:10.

Submit your next manuscript to BioMed Central and take full advantage of:

- **Convenient online submission**
- **Thorough peer review**
- **No space constraints or color figure charges**
- **Immediate publication on acceptance**
- **Inclusion in PubMed, CAS, Scopus and Google Scholar**
- **Research which is freely available for redistribution**

Submit your manuscript at
www.biomedcentral.com/submit

BioMed Central